Chemosphere 181 (2017) 232–240

Contents lists available at ScienceDirect

Chemosphere

journal homepage: www.elsevier.com/locate/chemosphere

Atmospheric degradation of 2-chloroethyl vinyl ether, allyl ether and allyl ethyl ether: Kinetics with OH radicals and UV photochemistry

M. Antiñolo [a, b], A.J. Ocaña [a], J.P. Aranguren [c], S.I. Lane [c], J. Albaladejo [a, b], E. Jiménez [a, b, *]

[a] Departamento de Química Física, Facultad de Ciencias y Tecnologías Químicas, Universidad de Castilla-La Mancha, Avda. Camilo José Cela, 1B, Ciudad Real, 13071, Spain

[b] Instituto de Investigación en Combustión y Contaminación Atmosférica, Universidad de Castilla-La Mancha, Camino de Moledores s/n, Ciudad Real, 13071, Spain

[c] Instituto de Investigaciones en Fisicoquímica de Córdoba, Departamento de Fisicoquímica, Facultad de Ciencias Químicas, Centro Láser de Ciencias Moleculares, Universidad Nacional de Córdoba, Ciudad Universitaria, Pabellón Argentina, Ala 1, Córdoba, 5000, Argentina

HIGHLIGHTS

- UV and IR absorption cross sections are reported for three unsaturated ethers.
- Rate coefficients of the OH-reaction of these unsaturated ethers are determined.
- A slightly negative activation energy is observed for k_{OH} between 263 and 358 K.
- OH-reaction, with a few hours lifetime, occurs in a greater extent than photolysis.
- Negligible contribution of these species to the global warming.

ARTICLE INFO

Article history:
Received 18 January 2017
Received in revised form
11 April 2017
Accepted 12 April 2017
Available online 18 April 2017

Handling Editor: R. Ebinghaus

Keywords:
Hydroxyl radicals
Unsaturated ethers
Tropospheric chemistry
Kinetics
Absorption cross sections

ABSTRACT

Unsaturated ethers are oxygenated volatile organic compounds (OVOCs) emitted by anthropogenic sources. Potential removal processes in the troposphere are initiated by hydroxyl (OH) radicals and photochemistry. In this work, we report for the first time the rate coefficients of the gas-phase reaction with OH radicals (k_{OH}) of 2-chloroethyl vinyl ether (2ClEVE), allyl ether (AE), and allyl ethyl ether (AEE) as a function of temperature in the 263–358 K range, measured by the pulsed laser photolysis–laser induced fluorescence technique. No pressure dependence of k_{OH} was observed in the 50–500 Torr range in He as bath gas, while a slightly negative T-dependence was observed. The temperature dependent expressions for the rate coefficients determined in this work are:

$$k_{OH,2ClEVE}(T) = (9.0\pm2.0) \times 10^{-12}\exp\left(\frac{478\pm72}{T}\right) \text{ cm}^3 \text{ molecule}^{-1} \text{ s}^{-1},$$

$$k_{OH,AE}(T) = (1.3\pm0.4) \times 10^{-11}\exp\left(\frac{442\pm91}{T}\right) \text{cm}^3 \text{ molecule}^{-1} \text{ s}^{-1},$$

$$k_{OH,AEE}(T) = (5.8\pm1.3) \times 10^{-12}\exp\left(\frac{563\pm62}{T}\right) \text{cm}^3 \text{ molecule}^{-1} \text{ s}^{-1},$$

The estimated atmospheric lifetimes (τ_{OH}) assuming k_{OH} at 288 K were 3, 2, and 4 h for 2ClEVE, AE and AEE, respectively. The kinetic results are discussed in terms of the chemical structure of the unsaturated ethers by comparison with similar compounds. We also report ultraviolet (UV) and infrared (IR) absorption cross sections (σ_λ and $\sigma(\tilde{\nu})$, respectively). We estimate the photolysis rate coefficients in the solar UV actinic region to be less than 10^{-7} s^{-1}, implying that these compounds are not removed from the atmosphere by this process. In addition, from $\sigma(\tilde{\nu})$ and τ_{OH}, the global warming potential of each

* Corresponding author. Departamento de Química Física, Facultad de Ciencias y Tecnologías Químicas, Universidad de Castilla-La Mancha, Avda. Camilo José Cela, 1B, Ciudad Real, 13071, Spain.
E-mail address: Elena.Jimenez@uclm.es (E. Jiménez).

http://dx.doi.org/10.1016/j.chemosphere.2017.04.053

unsaturated ether was calculated to be almost zero. A discussion on the atmospheric implications of the titled compounds is presented.

1. Introduction

Oxygenated volatile organic compounds (OVOCs) are an important group of trace gases in the troposphere. Their sources are biogenic or anthropogenic, or they may also be formed in the troposphere as secondary pollutants. They participate in several atmospheric processes, determining the oxidizing capacity of the atmosphere (Lewis et al., 2000; Singh et al., 2001).

Unsaturated ethers are OVOCs that are emitted anthropogenically, since they are used in different industries as solvents, motor oils additives, for the manufacturing of coatings or as intermediates for the synthesis of flavours, fragrances, and pharmaceuticals (The Merck Index, 2013). In particular, 2-chloroethyl vinyl ether (CH_2=$CHOCH_2CH_2Cl$, 2ClEVE) is used as precursor of polymers with diverse possible uses such as thickeners, solubilising agents, cross linking agents, flocculating agents, dispersants, adhesives, or binders (Eldin and Stockinger, 1980). 2ClEVE is also used in reactions in which hydroxyl (OH) groups must be protected (Sakatsume et al., 1991). Besides the uses of 2ClEVE in chemical synthesis, it has been detected in produced water in a petroleum site (Sirivedhin and Dallbauman, 2004). Another example is allyl ethyl ether (CH_2=$CHCH_2OCH_2CH_3$, AEE) that is used in the reaction with carbon monoxide to produce esters in the presence of a halide of group VII metal as catalyst (Hanes et al., 1987).

Due to their uses, unsaturated ethers may be released into the troposphere where the potential gas-phase removal processes are expected to be the reactions with OH and nitrate (NO_3) radicals, chlorine (Cl) atoms, and ozone (O_3). There are some experimental kinetic studies of many different unsaturated ethers with OH radicals (Perry et al., 1977; Thiault et al., 2002; Thiault and Mellouki, 2006; Zhou et al., 2006a, b, 2009, 2012; Peirone et al., 2011), with NO_3 (Scarfogliero et al., 2006; Zhou et al., 2006a,b, 2009, 2012), and with O_3 (Grosjean and Grosjean, 1998; Zhou et al., 2006a,b, 2009, 2012). Moreover, the reactivity between OH radicals and several vinyl ethers has been theoretically investigated as well (Han et al., 2014, 2015). Particularly, for 2ClEVE, allyl ether ((CH_2=$CHCH_2)_2O$, AE), and AEE scarce kinetic information is currently available in the literature. Peirone et al. (2011) reported the rate coefficients for the OH-reactions at room temperature and atmospheric pressure using a relative rate technique. To the best of our knowledge, no temperature dependence study on the OH-reactions with 2ClEVE (Reaction R1), AE (Reaction R2) and AEE (Reaction R3) has been performed to date.

$$OH + CH_2{=}CHOCH_2CH_2Cl \xrightarrow{k_{OH,2ClEVE}} Products, \quad (R1)$$

$$OH + (CH_2{=}CHCH_2)_2O \xrightarrow{k_{OH,AE}} Products, \quad (R2)$$

$$OH + CH_2{=}CHCH_2OCH_2CH_3 \xrightarrow{k_{OH,AEE}} Products \quad (R3)$$

Ultraviolet (UV) photolysis in the solar actinic region ($\lambda > 290$ nm) can also contribute to the atmospheric degradation of OVOCs. The gas-phase photochemistry of unsaturated ethers has not been widely investigated. For instance, for vinyl ethers the absorption cross sections (σ_λ) have been reported by Nieto-Gligorovski et al. (2009) between 190 and 227 nm. For this class of unsaturated ethers, the main absorption band appears below 200 nm with σ_λ on the order of 10^{-17} cm^2 molecule^{-1}, while the absorption decreases above 225 nm (σ_λ<10^{-21} cm^2 molecule^{-1}). Therefore, it is expected that unsaturated ethers are not removed from the troposphere by photolysis in the actinic region.

Another aspect of the potential impact of these emissions in the atmosphere is the absorption of infrared (IR) radiation that may affect the radiative forcing of climate change. The radiative efficiency (RE) of a species is usually calculated using radiative transfer models and accounting the strength and spectral position of the IR absorption bands, atmospheric structure, surface temperature, and presence or absence of clouds. Hence, to evaluate the contribution of unsaturated ethers to the radiative forcing of atmosphere, the IR absorption cross sections in the so-called IR atmospheric window (~8–14 μm) are needed. Peirone et al. (2011) reported the RE of 2ClEVE, AE, and AEE to be 0.0315, 0.0565, and 0.1294 W m^{-2} ppbv^{-1}, respectively. These authors derived the global warming potential (GWP) relative to CO_2 for these compounds using the simplified method described by Pinnock et al. (1995) to estimate the direct instantaneous cloudy-sky radiative forcing efficiency and the procedure proposed by Forster et al. (2007). Peirone et al. (2011) concluded that GWP for a time horizon (TH) of 20 years for 2ClEVE, AE, and AEE was 0.0121, 0.0245, and 0.1193, respectively, which is several orders of magnitude lower than those of other ethers like dimethyl ether (GWP = 1) or fluorinated ethers (GWP > 100) (ICCP, 2001).

The aim of this work is (*i*) to extend the OH-kinetic data for reactions (R1-R3) to temperatures of atmospheric interest, particularly below room temperature; (*ii*) to evaluate the importance of the photodegradation route for these unsaturated ethers with respect to the removal initiated by OH radicals; and (*iii*) to re-evaluate the contribution of 2ClEVE, AE, and AEE to the radiative forcing of climate change by accounting the atmospheric lifetime derived from the kinetic measurements as proposed by Hodnebrog et al. (2013).

For that purpose, we report the absolute rate coefficients of the reaction with the OH radical of 2ClEVE, AE, and AEE as a function of temperature in the range 263–358 K for the first time. The absolute kinetic technique of pulsed laser photolysis – laser induced fluorescence (PLP – LIF) was used to derive the rate coefficients k_{OH} at each temperature at pressures ranging between 50 and 500 Torr of He. A discussion on the structure-reactivity relationship is presented by comparison with similar compounds. The absolute k_{OH} at room temperature is compared to the relative one determined by Peirone et al. (2011). Additionally, the UV absorption cross sections between 200 and 350 nm were determined in this work for the first time. We also report the IR absorption cross sections for these unsaturated ethers between 500 and 4000 cm^{-1} at room temperature. The atmospheric lifetime and GWP of these unsaturated ethers were also estimated in order to discuss the atmospheric implications of the emission of these OVOCs.

2. Experimental procedure

Three different experimental systems were employed in this work: UV and FTIR absorption spectroscopy systems, and an OH radical kinetics set-up based on the PLP - LIF technique. All of them

have previously been described in detail (Jiménez et al., 2005; Antiñolo et al., 2010, 2014) and only a brief overview is given in the subsequent subsections.

2.1. UV and IR absorption spectroscopy systems

The UV and IR absorption spectroscopy systems have already been described in detail elsewhere (Jiménez et al., 2005; Antiñolo et al., 2010).

The UV spectroscopy set-up consists of a deuterium lamp (Oriel, emission range = 180–500 nm), an absorption cell (path length ℓ = 107 cm) and a spectrograph (Chromex) coupled to a charged coupled device (CCD) detector. The spectrograph uses a 300 grooves per mm grating centered at 290 nm which provides an instrumental resolution of 0.18 nm. The CCD is cooled at 253 K by a Peltier system to reduce the dark current and increase the signal-to-noise ratio. Wavelengths, ranging between 200 and 350 nm, were calibrated using a pen-ray Hg-Ar lamp (Newport). UV absorption spectra were recorded for the three unsaturated ethers in the gas phase at room temperature and at pressures between 2.6 and 9.2 Torr. Absorbance was measured as a function of wavelength (A_λ) as the natural logarithm of the ratio between the transmitted light intensity in the absence and presence of ether (I and I_0, respectively), and it is related to the absorption cross section (σ_λ) by means of the Beer-Lambert law:

$$A_\lambda = \ln\left(\frac{I_0}{I}\right)_\lambda = \sigma_\lambda \ell [R], \quad (1)$$

where [R] is the concentration of the unsaturated ether in molecule cm^{-3}. In Fig. S1 of the supplementary information, some examples of plots of A_λ versus [R] are shown at different wavelengths for all unsaturated ethers. Straight lines were obtained in all cases, accomplishing the Beer-Lambert law in the concentration range used. σ_λ were then determined from the slopes of these plots.

The IR spectroscopy system consists of a FTIR spectrometer (Bruker, Tensor 27) equipped with a Globar source and a mercury cadmium telluride (MCT) detector cooled with liquid N_2. Absorption spectra were measured at wavenumbers, $\tilde{\nu}$, between 500 and 4000 cm^{-1} with a 0.5-cm^{-1} resolution. Two different gas cells were used in independent measurements: a 10 cm-long cell and a variable multipass cell with a fixed path length of 800 cm. In the first one, vapour pressures (between 1.5 and 8.4 Torr) of the pure unsaturated ethers were introduced, whereas in the 800-cm long cell total pressures ranging 8 and 81 Torr of mixtures of ether (0.26–0.55%) and He were used. For each unsaturated ether 10–12 spectra were recorded at different concentrations. Beer-Lambert law (for wavenumbers in this case) was used again in order to get the IR absorption cross sections as a function of wavenumber, $\sigma(\tilde{\nu})$. In Fig. S2 of the supplementary information, some examples of plots of the absorbance versus [R] × ℓ (since different optical path lengths were used) are shown at different wavenumbers for all unsaturated ethers. In addition, integrated absorption cross sections (S_{int}), in base e, were also determined between 1500 and 500 cm^{-1} from the integrated absorbance (A_{int}, i.e. the area of a band between $\tilde{\nu}_1$ and $\tilde{\nu}_2$). S_{int} and A_{int} are defined as:

$$S_{int} = \int_{\tilde{\nu}_1}^{\tilde{\nu}_2} \sigma(\tilde{\nu}) d\tilde{\nu}, \quad (2)$$

$$A_{int} = \int_{\tilde{\nu}_1}^{\tilde{\nu}_2} A(\tilde{\nu}) d\tilde{\nu}, \quad (3)$$

Therefore, Eq. (1) is transformed into:

$$A_{int} = S_{int} \ell [R] \quad (4)$$

Straight lines were obtained in all cases, accomplishing the Beer-Lambert law in the concentration range used. S_{int} were then determined from the slopes of these plots.

2.2. OH radical kinetics set-up

The rate coefficients for reactions (1–3), k_{OH}, were determined by PLP – LIF as previously described elsewhere (Antiñolo et al., 2014). A jacketed Pyrex reaction cell, that was cooled or warmed by recirculating ethanol or water through the outer jacket, was used to get gas temperatures between 263 and 358 K. Helium was used as the bath gas, and the pressure inside the reaction cell ranged between 50 and 500 Torr. The total flow through the reactor (225–470 sccm, standard cubic centimeter per minute) was mainly formed by the flow of He with a small contribution (between 0.2 and 4.4%) of diluted unsaturated ether and the OH-precursor. Mixtures of the unsaturated ethers in He (f = 0.01–0.34% in the storage bulb) were flown through the reactor and further diluted with the bath gas, reaching concentrations between 1.3 × 10^{12} and 3.5 × 10^{14} molecule cm^{-3}. H_2O_2 and HNO_3 were used as aqueous solutions, and were introduced in the reaction cell by bubbling He through the solution. OH radicals were generated by photolysis of H_2O_2 or HNO_3 at 248 nm using a KrF excimer laser (E = 4.2–9.9 mJ $pulse^{-1}$ cm^{-2}, 10 Hz). H_2O_2 was used in the measurements at temperatures higher than room temperature and HNO_3 at lower temperatures. The OH-precursor concentrations in the reaction cell were estimated as described by Jiménez et al. (2007) to be (1.3–4.1) × 10^{14} and (1.1–4.4) × 10^{15} molecule cm^{-3}, for H_2O_2 and HNO_3, respectively. OH radicals were monitored as a function of reaction time by detecting the laser induced fluorescence (I_t) emitted at ca. 308 nm, after excitation to the upper electronic level at 282 nm. The excitation radiation was provided by a frequency-doubled dye laser working with Rhodamine 6G (Exciton) and pumped by a frequency-doubled Nd:YAG laser. A photomultiplier tube located orthogonally to the photolysis and excitation laser beams detected the LIF signal. Experiments were performed under *pseudo*-first order conditions, with unsaturated ethers concentrations typically higher than two orders of magnitude than initial [OH]. Under these conditions, the temporal profile of the LIF intensity (see some examples in Fig. S3) is given by:

$$I_t = I_0 e^{-k't}, \quad (5)$$

where I_t and I_0 are the LIF intensities at a time t (varying the delay between the photolysis and excitation lasers) and 0, respectively, and k' is the *pseudo*-first order rate coefficient, defined as:

$$k' = k_0 + k_{OH}[R], \quad (6)$$

k_0 is the rate coefficient determined when no unsaturated ether is present and it is due to the diffusion of OH out of the detection zone and the reaction between OH and its precursor (Antiñolo et al., 2012). k_{OH} at a single temperature and pressure was determined from the slope of the plots of k' *versus* [R].

2.3. Reagents

He (99.999%, Praxair) was used as supplied. 2ClEVE (99%), AE (98%), and AEE (95%) were purchased to Sigma-Aldrich, and were degassed by freeze-pump-thaw cycles prior to use. 2ClEVE contained 4-methoxyphenol (50 ppm) and 2,2′,2″-nitriloethanol (300 ppm) as stabilizers. HNO_3 (65%, Panreac) was used as supplied, and H_2O_2 (50%, Scharlau) was pre-concentrated by a flowing He through it for several days.

3. Results and discussion

3.1. Spectroscopic data

3.1.1. UV absorption cross sections

Fig. 1a illustrates the obtained UV spectrum in terms of σ_λ for 2ClEVE, AE, and AEE between 210 and 350 nm. An average uncertainty of 30% was found in σ_λ, which is caused by the low absorption of these ethers particularly above 240 nm. This uncertainty is around 20% at wavelengths below 240 nm. An example of the uncertainty is plotted in Fig. 1a for 2ClEVE at 235 nm. As it can be seen in Fig. 1a, in the investigated spectral region a decrease in the absorption is observed for all ethers, which corresponds to the tail of the $n \rightarrow \sigma^*$ and $\pi \rightarrow \pi^*$ transition bands of –O– and –C–C groups respectively. The observed decrease is steeper at wavelengths below ca. 240 nm, while at longer wavelengths it is milder. For AEE, a fine structure is observed between 240 and 260 nm, while no structure was observed for 2ClEVE and AE. This might be explained by the presence of an extra double bond. When compared the three unsaturated ethers, it is observed that σ_λ of 2ClEVE are higher than those for AEE and AE in the whole wavelength range. The reason for this is the presence of the vinyloxy (–O–C–C) group in 2ClEVE with a p-π conjugation that lowers the energy needed for the electronic transition.

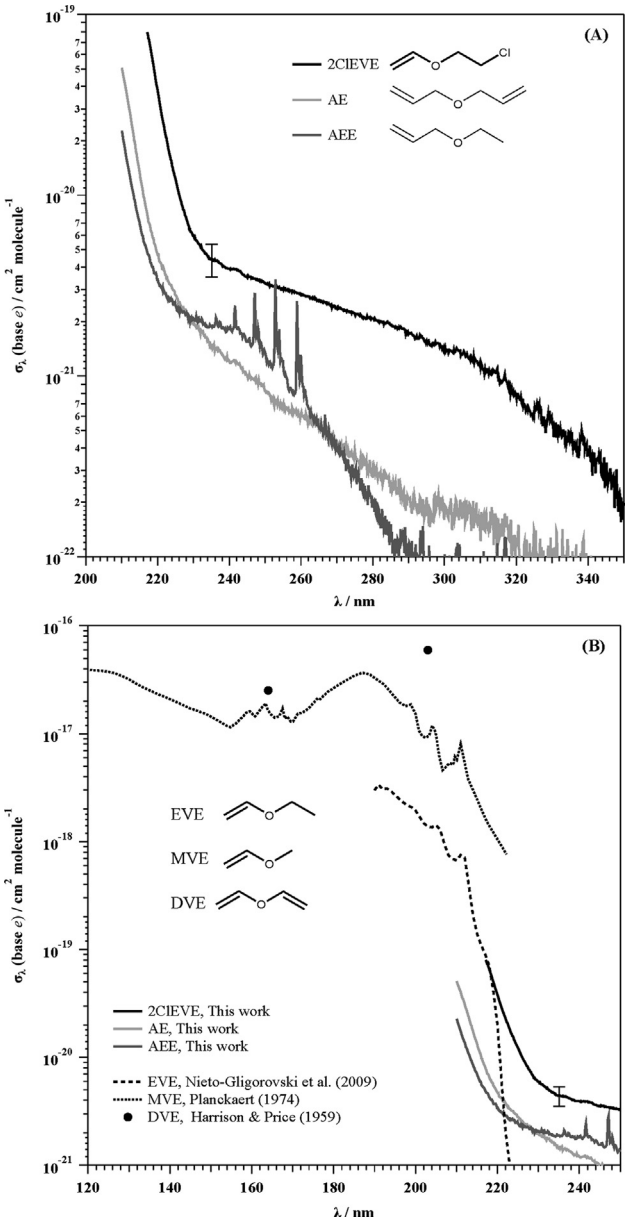

Fig. 1. (A) UV absorption cross sections (σ_λ) of the studied unsaturated ethers in this work. **(B)** UV-vacuum spectra of ethyl vinyl ether (EVE), methyl vinyl ether (MVE) and divinyl ether (DVE) are depicted for comparison purposes.

The absorption maximum of the $n \rightarrow \sigma^*$ and $\pi \rightarrow \pi^*$ bands, although not observed in this work due to instrumental limitations, might be located around 185–200 nm. The UV-vacuum absorption spectra for methyl vinyl ether (MVE) (Planckaert et al., 1974), ethyl vinyl ether (EVE) (Nieto-Gligorovski et al., 2009), and divinyl ether (DVE) (Harrison and Price, 1959) are depicted in Fig. 1b for comparison purposes. Only for MVE, the absorption peak is well-characterized at 186.9 nm. For EVE the absorption drastically decreases above 220 nm with respect to 2ClEVE. This may be due to the substitution of H by Cl, that can alter the spatial orientation of the vinyloxy system and therefore its polarization degree (Taskinen and Hellman, 1994; Taskinen, 1997), resulting in a change in the strength of the p-π conjugation.

3.1.2. IR absorption cross sections

Fig. 2 shows the IR spectra in terms of $\sigma(\tilde{\nu})$ for 2ClEVE, AE and AEE at room temperature. The IR spectra of the stabilizers 4-methoxyphenol and 2,2′,2″-nitriloethanol (NIST Mass Spec Data Center, 2009) were compared with the measured 2ClEVE spectrum, and no influence of these impurities was observed. A summary of the absorption cross sections of the main IR absorption peaks is shown in Table 1. The uncertainty is estimated to be ±6% taking into account the small variability of the different spectra recorded at several concentrations. The three unsaturated ethers present similar features such as the band corresponding to the C–O asymmetric stretching mode, located at 1100 and 1124 cm^{-1} in the AE and AEE spectra respectively, and at 1215 cm^{-1} in the 2ClEVE spectrum. This band is shifted to longer wavenumbers in the latter due to the conjugation of the vinyloxy system. The C=C stretching band also appears in the three spectra at 1625 cm^{-1} (2ClEVE), 1650 cm^{-1} (AE) or 1658 cm^{-1} (AEE), whereas the band at 824 cm^{-1} observed in the 2ClEVE spectrum is not seen in the two other spectra, being attributed to the C–Cl stretching. $\sigma(\tilde{\nu})$ of selected peaks are listed in Table 1 together with S_{int} in the 1500-500 cm^{-1} range. When our $\sigma(\tilde{\nu})$ are compared with those reported by Peirone et al. (2011), an incongruence is found in Fig. 5 of their paper, where the integrated absorption cross sections (*base 10*) are plotted, instead of $\sigma(\tilde{\nu})$ as stated. From a raw absorption spectrum provided by these authors, $\sigma(\tilde{\nu})$ are derived (data plotted in Fig. 2). For example, at 1099.8 cm^{-1} a difference of 12% is observed in the AE spectrum. As can be seen in Table 1, all S_{int} are on the order of 10^{-17} cm^2 molecule^{-1} cm^{-1}. Previously reported S_{int} for AE is similar to ours, whereas it is much higher for 2ClEVE and AEE. Considering the small difference in $\sigma(\tilde{\nu})$, S_{int} for 2ClEVE and AEE from Peirone et al. (2011) should be closer to the values listed in Table 1.

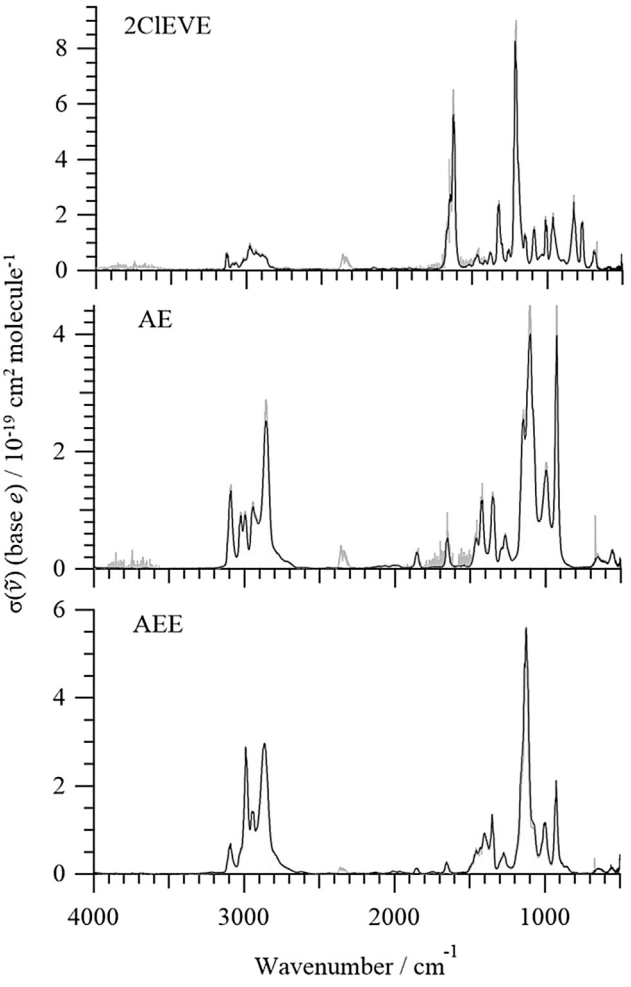

Fig. 2. IR absorption cross sections, $\sigma(\tilde{\nu})$, of 2ClEVE, AE, and AEE obtained in this work (black lines) together with the results obtained from the data sent on a personal communication by Peirone et al. (2011) (gray lines).

3.2. Kinetic data

Plots of k'-k_0 *versus* [R] are depicted in Fig. 3 for the studied unsaturated ethers at three different temperatures. k'-k_0 *versus* [R] is plotted instead of k' *versus* [R] in order to properly compare independent experiments by correcting the difference in measured k_0 (146-774 s^{-1}). The interval of k' was 890–21639 s^{-1} for 2ClEVE, 272 - 12107 s^{-1} for AE, and 973 - 14161 s^{-1} for AEE. As shown in Fig. 3, in all cases a decrease of the slope of such plots, that is k_{OH}, is observed as temperature is higher.

Experiments were performed under different pressure conditions, as shown in Table 2. No noticeable pressure dependence of k_{OH} was observed at a fixed temperature within the studied range, therefore an average k_{OH} is reported at each temperature (last column in Table 2).

Room temperature rate coefficient. As shown in Table 3, the average OH-rate coefficients for reactions (R1–R3) at 298 K are:

$$k_{OH,2ClEVE}(T = 298\ K) = (4.1\pm0.5) \times 10^{-11} cm^3\ molecule^{-1}\ s^{-1}$$

$$k_{OH,AE}(T = 298\ K) = (5.8\pm0.6) \times 10^{-11} cm^3\ molecule^{-1}\ s^{-1}$$

$$k_{OH,AEE}(T = 298\ K) = (3.7\pm0.6) \times 10^{-11} cm^3\ molecule^{-1}\ s^{-1}$$

The observed reactivity trend ($k_{OH,\ 2ClEVE} \sim k_{OH,\ AEE} < k_{OH,\ AE}$) is consistent with the proposed reaction mechanism for unsaturated ethers, where the predominant mechanism was reported to be the OH-addition to the double bond of the unsaturated ether, with a small contribution of the H-abstraction from the alkyl groups (Zhou et al., 2006b). It is then reasonable to obtain higher k_{OH} for AE than that for AEE, which presents only one allyl group. The experimental trend of k_{OH} is in excellent agreement with the calculated one by AOPWIN™ model (see Table 3). The relative kinetic study of Peirone et al. (2011) showed that $k_{OH,\ AEE} < k_{OH,\ AE}$. However, the OH-rate coefficient for reaction (R1) measured by these authors using a relative kinetic method is around twice the reported here and the estimate using AOPWIN™ model. The reason for such a discrepancy is unknown.

The effect of the presence of a double bond on k_{OH} is seen in Table 3. When the reactivity of 2-chloroethyl ethyl ether is compared with that of 2ClEVE, a decrease of 5 times in k_{OH} is observed (Dalmasso et al., 2010). The same trend is observed when comparing the OH-reactivity of AE and ethyl ether (Lloyd et al., 1976; Wallington et al., 1988, 1989; Bennett and Kerr, 1989; Bennett and Kerr, 1990; Nelson et al., 1990; Mellouki et al., 1995; Harry et al., 1999). The OH-reaction mechanism of saturated ethers is dominated by hydrogen abstraction, so the increase of reactivity when a double bond is introduced in the molecule may indicate that there is a contribution of the addition pathway. Our results also indicate that the substitution of an H atom in the methyl group of ethyl vinyl ether ($CH_3CH_2OCH{=}CH_2$) by a Cl atom greatly decreases the reactivity toward OH radicals. In contrast, Peirone et al. (2011) reported an increase in k_{OH} (see Table 3). Based on structure-reactivity trends, the substitution of an H atom of the hydrocarbon chain by a Cl atom in organic compounds tends to

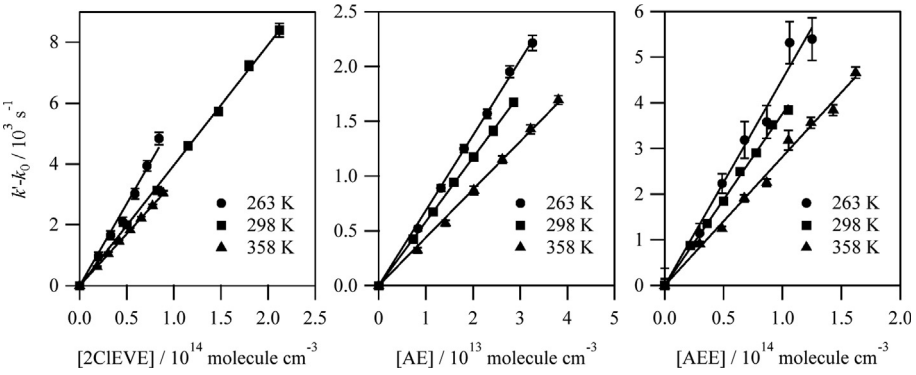

Fig. 3. Plots of k'-k_0 versus unsaturated ether concentration at three different temperatures.

Table 2
Summary of the experimental conditions and rate coefficients measured in this work under different pressure and temperature conditions.

	T/K	P/ Torr	E/mJ pulse^{-1} cm^{-2}	[R]/10^{13} molecule cm^{-3}	k_{OH} ± 2σ/ 10^{-11} cm^3 molecule^{-1} s^{-1}	Averaged k_{OH} ± 2σ/10^{-11} cm^3 molecule^{-1} s^{-1}
2ClEVE	263	72	4.9	2.0–8.4	5.7 ± 0.6	5.7 ± 0.4
		92	6.8	3.6–14	5.4 ± 0.9	
		300	6.7	9.7–35	5.8 ± 0.7	
	278	52	4.7	2.3–9.3	4.7 ± 0.2	4.8 ± 0.6
		71	6.8	1.9–8.0	5.0 ± 0.5	
		90	6.8	3.4–16	4.8 ± 0.4	
		301	5.7	9.3–33	5.7 ± 0.6	
	298	50	7.0	2.7–11	4.5 ± 0.3	4.1 ± 0.5
		60	6.3	2.7–13	4.4 ± 0.3	
		61	8.3	2.5–12	4.4 ± 0.5	
		71	6.6	4.0–19	4.9 ± 0.4	
		72	6.3	2.1–10	4.3 ± 0.9	
		96	5.2	4.2–13	3.9 ± 0.4	
		201	6.8	5.0–24	4.0 ± 0.1	
		303	6.8	6.1–24	4.2 ± 0.4	
	328	52	6.8	1.9–9.5	3.9 ± 0.2	3.9 ± 0.2
		92	5.7	3.6–17	4.0 ± 0.4	
		202	5.2	4.6–19	3.7 ± 0.3	
	358	53	5.4	1.8–8.9	3.4 ± 0.1	3.4 ± 0.1
		61	8.3	2.2–11	3.5 ± 0.1	
		206	6.8	4.3–21	3.2 ± 0.2	
AE	263	50	8.0	0.81–3.0	7.3 ± 0.3	7.1 ± 0.6
		80	5.2	4.2–16	7.6 ± 0.7	
		80	7.3	0.14–0.70	6.7 ± 0.4	
		300	7.6	0.85–3.9	6.8 ± 0.2	
		500	6.8	0.83–3.3	6.9 ± 0.2	
	278	50	8.4	0.77–3.0	6.7 ± 0.3	6.6 ± 0.3
		60	4.2	0.90–4.1	6.7 ± 0.3	
		120	8.9	0.81–3.7	6.4 ± 0.2	
		300	9.2	4.4–17	6.6 ± 0.6	
	298	50	9.9	0.43–2.0	6.2 ± 0.5	5.8 ± 0.6
		65	6.3	4.8–19	5.6 ± 0.5	
		70	7.8	0.13–0.53	5.6 ± 0.2	
		120	9.5	0.83–3.9	5.9 ± 0.2	
		300	9.4	0.73–2.9	5.8 ± 0.1	
		500	9.9	0.74–2.9	5.4 ± 0.3	
	328	50	8.8	0.77–3.0	5.3 ± 0.1	5.2 ± 0.2
		65	4.7	5.2–20	5.1 ± 0.4	
		120	7.3	0.90–4.2	5.1 ± 0.1	
		300	9.6	0.67–3.1	5.1 ± 0.3	
	358	50	8.5	0.57–2.6	4.7 ± 0.2	4.6 ± 0.6
		65	5.2	0.57–16	4.2 ± 0.3	
		120	7.2	0.82–3.8	4.5 ± 0.2	
		300	9.3	0.62–2.8	4.9 ± 0.3	
AEE	263	52	7.1	2.7–11	4.7 ± 0.4	4.8 ± 0.7
		94	7.6	3.8–18	4.2 ± 0.2	
		171	6.6	5.0–24	4.9 ± 0.1	
	278	55	7.6	2.5–11	4.3 ± 0.1	4.4 ± 0.1
		92	6.6	3.6–17	4.4 ± 0.1	
		144	7.8	5.7–24	4.4 ± 0.2	
	298	51	6.3	2.2–11	3.7 ± 0.1	3.7 ± 0.6
		70	7.6	2.9–13	3.8 ± 0.1	
		80	7.8	3.0–13	4.5 ± 0.3	
		102	5.9	2.8–13	3.9 ± 0.1	
		103	8.0	4.1–20	3.3 ± 0.1	
		211	6.9	5.6–27	3.4 ± 0.2	
		275	6.1	7.1–35	3.6 ± 0.2	
	328	51	6.3	2.0–9.6	3.3 ± 0.2	3.0 ± 0.3
		101	7.9	2.9–13	2.9 ± 0.1	
		105	8.3	3.9–14	3.2 ± 0.7	
		212	8.5	6.0–33	3.0 ± 0.1	
	358	52	6.3	1.8–8.8	2.9 ± 0.1	2.8 ± 0.1
		101	7.8	3.0–16	2.8 ± 0.2	
		196	8.1	5.1–28	2.8 ± 0.1	

Table 1
IR absorption cross sections (base *e*) at selected wavenumbers of the titled unsaturated ethers obtained in this work.

	Wavenumber/ cm^{-1}	$\sigma(\tilde{\nu})$/10^{-19} cm^2 molecule^{-1}	S_{int}/ 10^{-17}cm^2 molecule^{-1} cm^{-1}
2ClEVE	824.0	2.5	
	961.9	1.9	
	1214.6	8.3	
	1326.9	2.3	
	1625.4	5.6	
	1500–500		7.8 ± 0.2
AE	925.3	4.0	
	995.2	1.7	
	1099.8	4.0	
	1351.5	1.2	
	1427.7	1.2	
	2857.3	2.5	
	3095.5	1.3	
	1500–500		6.8 ± 0.1
AEE	924.3	2.1	
	1004.3	1.2	
	1123.4	5.6	
	1350.1	1.4	
	2864.5	3.0	
	2989.9	2.9	
	1500–500		6.1 ± 0.1

decrease the OH-rate coefficient (Atkinson et al., 2006, 2008). As Table 3 shows, it is observed a good agreement in the obtained $k_{OH,AE}$ (298 K) and $k_{OH,AEE}$ (298 K) in this work with previous results within the uncertainties.

Another aspect that can be observed is the effect of the –O– group on the OH-reactivity. The presence of the O atom on the OH-reactivity is small, since k_{OH}(298 K) for AE and AEE is barely affected when comparing with the corresponding alkenes, 1,5-hexadiene and 1-pentene, respectively. This behaviour is not observed for saturated species, as alkanes, which are much less reactive than their corresponding ethers (Atkinson and Arey, 2003), what indicates that the influence of the double bond is much more important than the influence of the O atom in the structure of the reactant towards the OH radical.

Temperature dependence of k_{OH}. It is seen in Table 1 that k_{OH} slightly decreases as T increases. The observed decrease in k_{OH} is around 60% between 263 and 358 K. Averaged OH-rate coefficients (in log scale) are plotted as a function of $1/T$ and fitted to the Arrhenius equation (Fig. 4), obtaining the following expressions:

$$k_{OH,2ClEVE}(T) = (9.0\pm2.0) \times 10^{-12}\exp\left(\frac{478\pm72}{T}\right)\text{cm}^3\ \text{molecule}^{-1}\ \text{s}^{-1}, \quad (7)$$

$$k_{OH,AE}(T) = (1.3\pm0.4) \times 10^{-11}\exp\left(\frac{442\pm91}{T}\right)\ \text{cm}^3\ \ \text{molecule}^{-1}\ \text{s}^{-1}, \quad (8)$$

$$k_{OH,AEE}(T) = (5.8\pm1.3) \times 10^{-12}\exp\left(\frac{563\pm62}{T}\right)\text{cm}^3\ \text{molecule}^{-1}\ \text{s}^{-1} \quad (9)$$

The obtained pre-exponential factor, A, and activation energy, E_a, are similar within the reported uncertainties (±2σ, statistical error). The slightly negative E_a, ranging from −4.7 to −3.7 kJ mol^{-1}, suggests that the reaction mechanism proceeds either by addition of the OH radical to the double bond of the unsaturated ether or by hydrogen-abstraction through a pre-reactive H-bonded complex.

Table 3
Comparison of kinetic parameters of the titled unsaturated ethers and other similar compounds.

Compound	k_{OH} (298 K)/10^{-11} cm^3 molecule^{-1} s^{-1}	A/10^{-12} cm^3 molecule^{-1} s^{-1}	(E_a/R)/K	Reference
2ClEVE ($ClCH_2CH_2OCH{=}CH_2$)	**4.1 ± 0.5**	**9.0 ± 2.0**	**−478 ± 72**	**This work**
	9 ± 1			Peirone et al. (2011)
	3.7			AOPWIN™ model
$CH_3CH_2OCH{=}CH_2$	7.79 ± 1.71			Zhou et al. (2006a)
	6.8 ± 0.7	1.55 ± 0.25	−445 ± 13	Thiault et al. (2002)
$ClCH_2CH_2OCH_2CH_3$	0.83 ± 0.19			Dalmasso et al. (2010)
AE ($(CH_2{=}CHCH_2)_2O$)	**5.8 ± 0.6**	**13 ± 4**	**−442 ± 91**	**This work**
	6.8 ± 0.7			Peirone et al. (2011)
	6.4			AOPWIN™ model
$CH_3CH_2CH_2OCH_2CH_2CH_3$	2.18 ± 0.17			Harry et al. (1999)
	2.16 ± 0.16	(1.84 ± 0.23) × $10^{-2}T^2$	−767 ± 34	Mellouki et al. (1995)
	1.99 ± 0.17			Nelson et al. (1990)
	1.86	11.5 ± 2.7	−144 ± 72	Bennett and Kerr (1990)
	1.53 ± 0.16			Bennett and Kerr (1989)
	1.97 ± 0.08			Wallington et al. (1989)
	1.80 ± 0.22	5.6 ± 1.7	−270 ± 100	Wallington et al. (1988)
	1.73 ± 0.35			Lloyd et al. (1976)
$CH_2{=}CHCH_2CH_2CH{=}CH_2$	5.85 ± 0.35			Ohta (1983)
AEE ($CH_3CH_2OCH_2CH{=}CH_2$)	**3.7 ± 0.6**	**5.8 ± 1.3**	**−563 ± 62**	**This work**
	4.2 ± 0.7			Peirone et al. (2011)
	3.7			AOPWIN™ model
$CH_3CH_2CH_2CH{=}CH_2$	2.74 ± 0.38	1.07 ± 0.62	−1016 ± 129	McGillen et al. (2007)
	3.13 ± 0.13			Atkinson and Aschmann (1984)
	2.9 ± 0.4			Biermann et al. (1982)
	3.97 ± 0.38			Nip and Paraskevopoulos (1979)

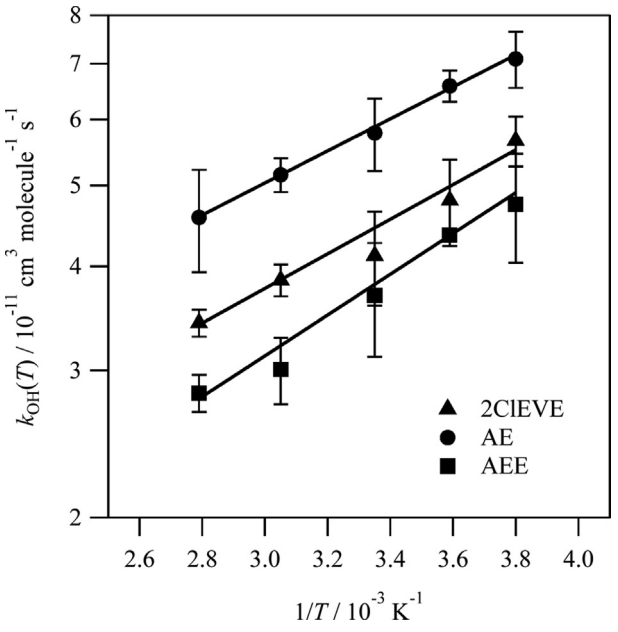

Fig. 4. Arrhenius plot for the studied unsaturated ethers.

The addition mechanism was observed to be predominant for the reaction between propyl vinyl ether and OH, in which the formation of propyl formate and formaldehyde was observed with yields between 60 and 80% (Zhou et al., 2006b). It was also proposed a small contribution (11%) of the H-abstraction from the alkyl groups. For the OH + EVE reaction, with a suggested addition mechanism of the OH radical to the double bond, a similar E_a was also reported (see Table 3) (Thiault et al., 2002). For the OH-reaction with saturated ethers, such as propyl ether, the reported activation energy is also negative, but in this case, the proposed mechanism is an indirect H-abstraction pathway via the formation of an OH … ether adduct (Nelson et al., 1990; Mellouki et al., 1995), similarly to what was observed for other oxygenated VOCs such as acetone (Vandenberk et al., 2002). As shown in Table 3, the variability of E_a for propyl ether makes impossible to establish a good trend for this parameter. Although no product study is available to confirm which mechanism is taking place in the reaction between OH radicals and the title unsaturated ethers, based on previous studies on saturated and unsaturated ethers, it looks very likely that the reaction will mainly proceed via an OH-addition to the double bond with a small contribution of H-abstraction through the formation of a pre-reactive complex.

4. Atmospheric implications

In the UV solar actinic region (λ > 290 nm), region of atmospheric interest, the title compounds present a very low absorption (< 2 × 10^{-21} cm^2 molecule^{-1} for 2ClEVE; < 2 × 10^{-22} cm^2 molecule^{-1} for AE; < 10^{-22} cm^2 molecule^{-1} for AEE). From the UV absorption cross sections derived in this work, the estimation of the photolysis rate coefficient, J, can be made by following the same method previously described by our group (Antiñolo et al., 2011). The photolysis quantum yield has been considered to be 1 and the solar actinic spectral flux of a sunny midday of June in Ciudad Real was taken from the Tropospheric Ultraviolet Visible (TUV) model (Madronich and Flocke, 1999). With these considerations, we have estimated an upper limit of J < 3 × 10^{-6} s^{-1} for 2ClEVE, J < 3 × 10^{-7} s^{-1} for AE, and J < 1 × 10^{-7} s^{-1} for AEE. Therefore, the tropospheric lifetimes of the titled compounds due to photodegradation ($\tau_{hv} = 1/J$) were estimated to be > 4 days for 2ClEVE, > 1 month for AE, and > 4 months for AEE.

Regarding the tropospheric lifetime (τ_{Oxid}) of 2ClEVE, AE and AEE due to homogeneous processes initiated by reaction with tropospheric oxidants (OH and NO_3 radicals, O_3, or Cl atoms), it can be estimated assuming an average concentration of the oxidant in the atmosphere ([Oxid]) and that the unsaturated ether is uniformly distributed in the troposphere:

$$\tau_{Oxid} = \frac{1}{k_{Oxid}[Oxid]}, \quad (10)$$

For the OH reaction, the lifetime τ_{OH} was estimated using

k_{OH}(288 K) determined from the Arrhenius expression obtained in this work, since 288 K is the average temperature in the Earth surface, and $[OH]_{12h} = 1.9 \times 10^6$ radical cm^{-3} reported by Prinn et al. (2001) as the average concentration of OH in the atmosphere during daytime. The estimated τ_{OH} was ca. 3, 2, and 4 h for 2ClEVE, AE, and AEE, respectively, implying that these compounds will be oxidized very rapidly near the emission sources. It is clear that atmospheric UV photolysis of these ethers is negligible compared with the removal initiated by reaction with the OH radical.

It is interesting to compare the contribution of other degradation routes to the disappearance of the studied unsaturated ethers. The availability of kinetic data for the reaction of these compounds with other tropospheric oxidants is very scarce. As far as we know, only the reaction of AEE with O_3 is reported in the literature, with a rate coefficient $k_{O3,\ AEE} = 8.69 \times 10^{-18}$ cm^3 $molecule^{-1}$ s^{-1} (Al Mulla et al., 2010). Assuming an average O_3 concentration, $[O_3]_{24h} = 7 \times 10^{11}$ molecule cm^{-3} (Logan, 1985), $\tau_{O3,\ AEE}$ is estimated to be ca. 2 days, indicating that the OH radical reaction is a more important degradation route for AEE than reaction with O_3. For other vinyl ethers, such as *iso*-butyl and *tert*-butyl vinyl ethers, Zhou et al. (2012) found out that the tropospheric lifetimes due to their reaction with OH, NO_3 and O_3 were very similar, ranging the lifetimes for the individual processes between 1 and 2 h (they considered the 12-h daytime average concentration of OH and the 12-h night time concentration of NO_3). In that case, OH and O_3 compete for the daytime removal of these vinyl ethers. To our knowledge, no kinetic data on NO_3 and Cl reactions with the investigated unsaturated ethers here has been reported yet. Based on the behaviour of other unsaturated ethers, it is expected that for 2ClEVE, AE, and AEE these degradation routes may have comparable importance. Further kinetic studies with those oxidants are needed to confirm this.

The contribution of the 2ClEVE, AE and AEE to the climate change can be evaluated by calculating their GWP. In this work, we followed the method proposed by Hodnebrog et al. (2013), in which a correction is made for short-lived species (lifetimes shorter than 0.5 years). This correction makes that the calculated GWP(TH = 20 years) for the title unsaturated ethers are lower than 2×10^{-3}, even lower to what was found by Peirone et al. (2011), confirming that these compounds do not have any impact on global warming.

5. Conclusions

In this work, we reported UV and IR absorption cross sections for the unsaturated ethers 2ClEVE, AE, and AE at room temperature. No absorption in the UV solar actinic region ($\lambda > 290$ nm) is expected, consequently the estimated photolysis rate coefficients are very low, on the order of 10^{-6} - 10^{-7} s^{-1}. We have determined for the first time the rate coefficients of the reaction between OH radicals and 2ClEVE, AE, and AEE as a function of temperature in the range between 263 and 358 K and at different pressures of He in the interval 50–500 Torr. No pressure dependence was observed in the studied range, whereas a slightly negative temperature dependence of k_{OH} was noticed, this suggests that the mechanism proceeds either by addition of the OH radical to the double bond or by H-abstraction after the formation of a pre-reactive OH … ether adduct.

The lifetimes of the studied unsaturated ethers point out that, once emitted, they will be removed in a few hours, being reaction with OH radicals a more important degradation route than photolysis, although it looks feasible that reaction with other tropospheric oxidants may compete under certain circumstances. Finally, we concluded that these compounds are not expected to have any effect on the global warming of Earth's atmosphere.

Acknowledgements

Authors would like to acknowledge the Spanish Ministry of Economy and Competitiveness and the Regional government of Castilla-La Mancha for supporting this work under the GASSOL project (CGL2013-43227-R) and the FOTOCINE project (PEII-2014-043-P). M. Antiñolo also wants to thank University of Castilla-La Mancha (Plan Propio de Investigación) for funding.

Appendix A. Supplementary data

Supplementary data related to this article can be found at http://dx.doi.org/10.1016/j.chemosphere.2017.04.053.

References

Al Mulla, I., Viera, L., Morris, R., Sidebottom, H., Treacy, J., Mellouki, A., 2010. Kinetics and mechanisms for the reactions of ozone with unsaturated oxygenated compounds. ChemPhysChem 11, 4069–4078.
Antiñolo, M., Jiménez, E., Notario, A., Martínez, E., Albaladejo, J., 2010. Tropospheric photooxidation of CF_3CH_2CHO and $CF_3(CH_2)_2CHO$ initiated by Cl atoms and OH radicals. Atmos. Chem. Phys. 10, 1911–1922.
Antiñolo, M., Jiménez, E., Albaladejo, J., 2011. UV absorption cross sections between 230 and 350 nm and pressure dependence of the photolysis quantum yield at 308 nm of CF_3CH_2CHO. Phys. Chem. Chem. Phys. 13, 15936–15946.
Antiñolo, M., González, S., Ballesteros, B., Albaladejo, J., Jiménez, E., 2012. Laboratory studies of $CHF_2CF_2CH_2OH$ and $CF_3CF_2CH_2OH$: UV and IR absorption cross sections and OH rate coefficients between 263 and 358 K. J. Phys. Chem. A 116, 6041–6050.
Antiñolo, M., Jiménez, E., González, S., Albaladejo, J., 2014. Atmospheric chemistry of CF_3CF_2CHO: absorption cross sections in the UV and IR regions, photolysis at 308 nm, and gas-phase reaction with OH radicals (T = 263–358 K). J. Phys. Chem. A 118, 178–186.
Atkinson, R., Arey, J., 2003. Atmospheric degradation of volatile organic compounds. Chem. Rev. 103, 4605–4638.
Atkinson, R., Aschmann, S.M., 1984. Rate constants for the reaction of OH radicals with a series of alkenes and dialkenes at 295 ± 1 K. Int. J. Chem. Kinet. 16, 1175–1186.
Atkinson, R., Baulch, D.L., Cox, R.A., Crowley, J.N., Hampson, R.F., Hynes, R.G., Jenkin, M.E., Rossi, M.J., Troe, J., 2006. Evaluated kinetic and photochemical data for atmospheric chemistry: volume II - gas phase reactions of organic species. Atmos. Chem. Phys. 6, 3625–4055.
Atkinson, R., Baulch, D.L., Cox, R.A., Crowley, J.N., Hampson, R.F., Hynes, R.G., Jenkin, M.E., Rossi, M.J., Troe, J., Wallington, T.J., 2008. Evaluated kinetic and photochemical data for atmospheric chemistry: volume IV – gas phase reactions of organic halogen species. Atmos. Chem. Phys. 8, 4141–4496.
Bennett, P.J., Kerr, J.A., 1989. Kinetics of the reactions of hydroxyl radicals with aliphatic ethers studied under simulated atmospheric conditions. J. Atmos. Chem. 8, 87–94.
Bennett, P.J., Kerr, J.A., 1990. Kinetics of the reactions of hydroxyl radicals with aliphatic ethers studied under simulated atmospheric conditions: temperature dependences of the rate coefficients. J. Atmos. Chem. 10, 27–38.
Biermann, H.W., Harris, G.W., Pitts, J.N., 1982. Photoionization mass spectrometer studies of the collisionally stabilized product distribution in the reaction of hydroxyl radicals with selected alkenes at 298 K. J. Phys. Chem. 86, 2958–2964.
Dalmasso, P.R., Taccone, R.A., Nieto, J.D., Cometto, P.M., Lane, S.I., 2010. Kinetic study of the OH reaction with some hydrochloroethers under simulated atmospheric conditions. Atmos. Environ. 44, 1749–1753.
Eldin, S.H., Stockinger, F., 1980. Vinyl ethers, process for their preparation, and their use for the preparation of polymers. In: Patent, U.S. (Ed.). Ciba-Geigy Corporation, United States, 11.
Forster, P., Ramaswamy, V., Artaxo, P., Berntsen, T., Betts, R., Fahey, D.W., Haywood, J., Lean, J., Lowe, D.C., Myhre, G., Nganga, J., Prinn, R., Raga, G., Schulz, M., Van Dorland, R., 2007. Changes in atmospheric constituents and in radiative forcing. In: Solomon, S., Qin, D., Manning, M., Chen, Z., Marquis, M., Averyt, K.B., Tignor, M., Miller, H.L. (Eds.), Climate Change 2007: the Physical Science Basis. Contribution of Working Group I to the Fourth Assessment Report of the Intergovernmental Panel on Climate Change. Cambridge University Press, Cambridge, UK, and New York, USA.
Grosjean, E., Grosjean, D., 1998. Rate constants for the gas-phase reaction of ozone with unsaturated oxygenates. Int. J. Chem. Kinet. 30, 21–29.
Han, D.D., Cao, H.J., Li, J., Li, M.Y., He, M.X., Hu, J.T., 2014. Computational study on the mechanisms and rate constants of the OH-initiated oxidation of ethyl vinyl ether in atmosphere. Chemosphere 111, 61–69.
Han, D.D., Cao, H.J., Li, J., Li, M.Y., Li, X., He, M.X., Hu, J.T., 2015. Theoretical studies on the mechanisms and rate constants for the hydroxylation of n-butyl, iso-butyl and tert-butyl vinyl ethers in atmosphere. Struct. Chem. 26, 713–729.
Hanes, R.M., Jack, K., Thomas, S.B., 1987. Carbonylation of allylic ethers to esters. In: Office, E.P. (Ed.), Patentanwälte Grünecker, Kinkeldey, Stockmair & Partner, p. 8.
Harrison, A.J., Price, D.R.W., 1959. Absorption of acyclic oxygen compounds in the

vacuum ultraviolet. II. Ethers. J. Chem. Phys. 30, 357–360.
Harry, C., Arey, J., Atkinson, R., 1999. Rate constants for the reactions of OH radicals and Cl atoms with Di-n-Propyl ether and Di-n-Butyl ether and their deuterated analogs. Int. J. Chem. Kinet. 31, 425–431.
Hodnebrog, Ø., Etminan, M., Fuglestvedt, J.S., Marston, G., Myhre, G., Nielsen, C.J., Shine, K.P., Wallington, T.J., 2013. Global warming potentials and radiative efficiencies of halocarbons and related compounds: a comprehensive review. Rev. Geophys. 51, 300–378.
ICCP, 2001. In: Houghton, J.T., Ding, Y.J.G.D., Noguer, M., van der Linden, P.J., Dai, X., Maskell, K., Johnson, C.A. (Eds.), Climate Change 2001: the Scientific Basis: Contribution of Working Group 1 to the Third Assessment Report of the Intergovernmental Panel on Climate Change, p. 881. Cambridge, United Kingdom and New York, NY, USA.
Jiménez, E., Lanza, B., Garzón, A., Ballesteros, B., Albaladejo, J., 2005. Atmospheric degradation of 2-butanol, 2-Methyl-2-butanol, and 2,3-Dimethyl-2-butanol: OH kinetics and UV absorption cross sections. J. Phys. Chem. A 109, 10903–10909.
Jiménez, E., Lanza, B., Martínez, E., Albaladejo, J., 2007. Daytime tropospheric loss of hexanal and trans-2-hexenal: OH kinetics and UV photolysis. Atmos. Chem. Phys. 7, 1565–1574.
Lewis, A.C., Carslaw, N., Marriott, P.J., Kinghorn, R.M., Morrison, P., Lee, A.L., Bartle, K.D., Pilling, M.J., 2000. A larger pool of ozone-forming carbon compounds in urban atmospheres. Nature 405, 778–781.
Lloyd, A.C., Darnall, K.R., Winer, A.M., Pitts, J.N., 1976. Relative rate constants for the reactions of OH radicals with isopropyl alcohol, diethyl and DI-n-propyl ether at 305 ± 2 K. Chem. Phys. Lett. 42, 205–209.
Logan, J.A., 1985. Tropospheric ozone: seasonal behavior, trends, and anthropogenic influence. J. Geophys. Res. Atmos. 90, 10463–10482.
Madronich, S., Flocke, S., 1999. The role of solar radiation in atmospheric chemistry. In: Boule, P. (Ed.), Environmental Photochemistry. Springer Berlin Heidelberg, Berlin, Heidelberg, pp. 1–26.
McGillen, M.R., Percival, C.J., Shallcross, D.E., Harvey, J.N., 2007. Is hydrogen abstraction an important pathway in the reaction of alkenes with the OH radical? Phys. Chem. Chem. Phys. 9, 4349–4356.
Mellouki, A., Teton, S., Le Bras, G., 1995. Kinetics of OH radical reactions with a series of ethers. Int. J. Chem. Kinet. 27, 791–805.
Nelson, L., Rattigan, O., Neavyn, R., Sidebottom, H., Treacy, J., Nielsen, O.J., 1990. Absolute and relative rate constants for the reactions of hydroxyl radicals and chlorine atoms with a series of aliphatic alcohols and ethers at 298 K. Int. J. Chem. Kinet. 22, 1111–1126.
Nieto-Gligorovski, L.I., Gligorovski, S., Romano, R., Védova, C.D., Zetzsch, C., 2009. UV absorption cross-sections of a series of vinyl ethers. J. Photochem. Photobiol. A Chem. 204, 46–51.
Nip, W.S., Paraskevopoulos, G., 1979. Rates of OH radical reactions. VI. Reactions with C_3H_6, 1-C_4H_8 and 1-C_5H_{10} at 297 K. J. Chem. Phys. 71, 2170–2174.
NIST Mass Spec Data Center, S.E.S., director, 2009. Infrared spectra. In: Linstrom, P.J., Mallard, W.G. (Eds.), NIST Chemistry WebBook, NIST Standard Reference Database Number 69. National Institute of Standards and Technology, Gaithersburg MD, p. 20899.
Ohta, T., 1983. Rate constants for reactions of diolefins with hydroxyl radicals in the gas phase. Estimate of the rate constants from those for monoolefins. J. Phys. Chem. 87, 1209–1213.
Peirone, S.A., Aranguren Abrate, J.P., Taccone, R.A., Cometto, P.M., Lane, S.I., 2011. Kinetic study of the OH-initiated photo-oxidation of four unsaturated (allyl and vinyl) ethers under simulated atmospheric conditions. Atmos. Environ. 45, 5325–5331.
Perry, R.A., Atkinson, R., Pitts, J.N., 1977. Rate constants for the reaction of OH radicals with dimethyl ether and vinyl methyl ether over the temperature range 299–427 °K. J. Chem. Phys. 67, 611–614.
Pinnock, S., Hurley, M.D., Shine, K.P., Wallington, T.J., Smyth, T.J., 1995. Radiative forcing of climate by hydrochlorofluorocarbons and hydrofluorocarbons. J. Geophys. Research Atmospheres 100, 23227–23238.
Planckaert, A.A., Doucet, J., Sandorfy, C., 1974. Comparative study of the vacuum ultraviolet absorption and photoelectron spectra of some simple ethers and thioethers. J. Chem. Phys. 60, 4846–4853.
Prinn, R.G., Huang, J., Weiss, R.F., Cunnold, D.M., Fraser, P.J., Simmonds, P.G., McCulloch, A., Harth, C., Salameh, P., O'Doherty, S., Wang, R.H.J., Porter, L., Miller, B.R., 2001. Evidence for substantial variations of atmospheric hydroxyl radicals in the past two decades. Science 292, 1882–1888.
Sakatsume, O., Yamaguchi, T., Ishikawa, M., Hirao, I., Miura, K.-i., Takaku, H., 1991. Solid phase synthesis of oligoribonucleotides by the phosphoramidite approach using 2′-O-1-(2-chloroethoxy)ethyl protection. Tetrahedron 47, 8717–8728.
Scarfogliero, M., Picquet-Varrault, B., Salce, J., Durand-Jolibois, R., Doussin, J.-F., 2006. Kinetic and mechanistic study of the gas-phase reactions of a series of vinyl ethers with the nitrate radical. J. Phys. Chem. A 110, 11074–11081.
Singh, H., Chen, Y., Staudt, A., Jacob, D., Blake, D., Heikes, B., Snow, J., 2001. Evidence from the Pacific troposphere for large global sources of oxygenated organic compounds. Nature 410, 1078–1081.
Sirivedhin, T., Dallbauman, L., 2004. Organic matrix in produced water from the osage-skiatook petroleum environmental research site, osage county, Oklahoma. Chemosphere 57, 463–469.
Taskinen, E., 1997. ^{17}O NMR Spectra of divinyl ethers. Magn. Reson. Chem. 35, 107–110.
Taskinen, E., Hellman, J., 1994. ^{17}O NMR spectra of vinyl ethers. Magn. Reson. Chem. 32, 353–357.
The Merck Index, 2013, 15th edition ed. Royal Society of Chemistry, Cambridge, UK.
Thiault, G., Mellouki, A., 2006. Rate constants for the reaction of OH radicals with n-propyl, n-butyl, iso-butyl and tert-butyl vinyl ethers. Atmos. Environ. 40, 5566–5573.
Thiault, G., Thevenet, R., Mellouki, A., Le Bras, G., 2002. OH and O_3-initiated oxidation of ethyl vinyl ether. Phys. Chem. Chem. Phys. 4, 613–619.
Vandenberk, S., Vereecken, L., Peeters, J., 2002. The acetic acid forming channel in the acetone + OH reaction: a combined experimental and theoretical investigation. Phys. Chem. Chem. Phys. 4, 461–466.
Wallington, T.J., Liu, R., Dagaut, P., Kurylo, M.J., 1988. The gas phase reactions of hydroxyl radicals with a series of aliphatic ethers over the temperature range 240–440 K. Int. J. Chem. Kinet. 20, 41–49.
Wallington, T.J., Andino, J.M., Skewes, L.M., Siegl, W.O., Japar, S.M., 1989. Kinetics of the reaction of OH radicals with a series of ethers under simulated atmospheric conditions at 295 K. Int. J. Chem. Kinet. 21, 993–1001.
Zhou, S., Barnes, I., Zhu, T., Bejan, I., Benter, T., 2006a. Kinetic study of the gas-phase reactions of OH and NO_3 radicals and O_3 with selected vinyl ethers. J. Phys. Chem. A 110, 7386–7392.
Zhou, S., Barnes, I., Zhu, T., Klotz, B., Albu, M., Bejan, I., Benter, T., 2006b. Product study of the OH, NO_3, and O_3 initiated atmospheric photooxidation of propyl vinyl ether. Environ. Sci. Technol. 40, 5415–5421.
Zhou, S., Barnes, I., Zhu, T., Benter, T., 2009. Rate coefficients for the gas-phase reactions of OH and NO_3 radicals and O_3 with ethyleneglycol monovinyl ether, ethyleneglycol divinyl ether, and diethyleneglycol divinyl ether. J. Phys. Chem. A 113, 858–865.
Zhou, S., Barnes, I., Zhu, T., Benter, T., 2012. Kinetic study of gas-phase reactions of OH and NO_3 radicals and O_3 with iso-butyl and tert-butyl vinyl ethers. J. Phys. Chem. A 116, 8885–8892.